Published in "Supramolecular Chemistry 26(2): 125–137, 2014"
which should be cited to refer to this work.

Supporting Information

Influence of linear and branched perfluoroalkylated side chains on the π–π stacking behaviour of hexa–peri–hexabenzocoronene and thermotropic properties

Bassam Alameddine[a*], Olivier Frédéric Aebischer[b], Benoît Heinrich[c], Daniel Guillon[c], Bertrand Donnio[c*] and Titus A. Jenny[d*]

[a]*Department of Mathematics and Natural Sciences, Gulf University for Science and Technology, Hawally 32093, Kuwait.*

[b]*BASF Pharma (Evionnaz) SA, G–ENP/OD, Route du Simplon 1, CH–1902 Evionnaz, Valais, Switzerland.*

[c]*Institut de Physique et Chimie des Matériaux de Strasbourg (IPCMS), UMR 7504 (CNRS–Université de Strasbourg), 23 rue du Loess, BP43, 67034, Strasbourg cedex 2, France.*

[d]*Chemistry Department, University of Fribourg, Chemin du Musée 9, CH–1700 Fribourg, Switzerland.*

Email: titus.jenny@unifr.ch

d Corresponding author

Tables of indexation, and phase's parameters
X-ray diffraction patterns (A), and electronic density charts (B)
Thermogravimetry curves
Molecular dynamic simulation
Cryo-SEM data

Table S1. Table of indexation of the HBC derivatives

HBC	d_{exp} [Å][a]	[hk][b]	Intensity[c]	d_{theo} [Å][a,d]	Parameters at T = 200°C[d,e]
HBC-$(R_{4,4})_6$	23.1	10	VS (sh)	23.0_5	a = 26.6 Å
	13.4	11	S (sh)	13.3	S = 615 Å^2
	11.5	20	S (sh)	11.5	V_{mol} = 2525 Å^3
	8.7	21	M (sh)	8.7	
	7.4	$2h_0$	W (br)	-	
	5.4_5	h_F+h_H	VS (br)	5.4_5	
	3.7	h_0	W (br)	4.1	
HBC-$(R_{8,4})_6$	29.0	-	VS (br)	-	V_{mol} = 3260 Å^3
	14.9	-	S (br)	-	
	5.4	h_F+h_H	VS (br)	5.2_5	
	3.6	h_0	W (br)	-	
HBC-$(R_{2,6})_6$	25.2	10	VS (sh)	24.9	a = 28.7_5 Å
	12.3_5	20	W (sh)	12.4_5	S = 716 Å^2
	9.3_5	21	M (sh)	9.4	V_{mol} = 2725 Å^3
	7.3	$2h_0$	W (br)	-	
	5.6	h_F+h_H	VS (br)	5.6_5	
	3.6_5	h_0	W (br)	3.8	
HBC-$(R_{3,6})_6$	27.1	10	VS (sh)	26.8_5	a = 31.0 Å
	13.4_5	20	S (sh)	13.4_5	S = 832 Å^2
	10.1	21	S (sh)	10.1_5	V_{mol} = 2910 Å^3
	7.7	22	W (sh)	7.7_5	
	7.4_5	31	M (sh)	7.4_5	
	5.7	h_F+h_H	VS (br)	5.6	
	3.5_5	h_0	S (sh)	3.5	
HBC-$(R_{4,6})_6$	27.2_5	10	VS (sh)	27.2	a = 31.4 Å
	15.7_5	11	W (sh)	15.7	S = 854 Å^2
	13.5_5	20	S (sh)	13.6	V_{mol} = 3100 Å^3
	10.3	21	S (sh)	10.3	
	7.8_5	22	W (sh)	7.8_5	
	7.5_5	31	W (sh)	7.5_5	
	5.6_5	h_F+h_H	VS (br)	5.5_5	
	3.5	h_0	S (sh)	3.6	
HBC-$(R_{5,6})_6$	29.3	10	VS (sh)	29.1	a = 33.6 Å
	16.7_5	11	S (sh)	16.8	S = 978 Å^2
	14.5	20	VS (sh)	14.5_5	V_{mol} = 3275 Å^3
	11.0	21	M (sh)	11.0	
	7.0	$2h_0$	VW (br)	-	
	5.5_5	h_F+h_H	VS (br)	5.4_5	
	3.5	h_0	S (sh)	3.3_5	
HBC-$(R_{6,6})_6$	29.1_5	10	VS (sh)	29.0	a = 33.5 Å
	16.6_5	11	S (sh)	16.7_5	S = 971 Å^2
	14.5	20	S (sh)	14.5	V_{mol} = 3460 Å^3
	10.9_5	21	M (sh)	11.0	
	7.0	$2h_0$	VW (br)	-	
	5.6	h_F+h_H	VS (br)	5.4_5	
	3.5	h_0	S (sh)	3.5_5	
HBC-$(R_{8,6})_6$	15.6	-	S (br)	-	V_{mol} = 3830 Å^3
	5.4	h_F+h_H	VS (br)	5.3_5	
	3.6	h_0	W (br)	-	
HBC-$(R_{2,8})_6$	27.2	20/11	M (sh)	27.2	a = 54.4, b = 31.4
	15.7	31	M (sh)	15.7	S = 854 Å^2
	12.3	41	M (sh)	12.5	(a = 31.4)
	10.3	42/51/13	W (sh)	10.3	V_{mol} = 3300 Å^3
	7.3	$2h_0$	W (br)	-	
	5.8	h_F+h_H	VS (br)	5.7	
	3.7	h_0	M (sh)	3.8_5	
HBC-$(R_{3,8})_6$	29.3_5	10	M (sh)	29.2	a = 33.7 Å

	14.6	20	M (sh)	14.6	S = 984 Å^2
	10.9_5	21	S (sh)	11.0_5	V_{mol} = 3480 Å^3
	5.6_5	h_F+h_H	VS (br)	5.6_5	
	3.5_5	h_0	S (sh)	3.5	
HBC-$(R_{4,8})_6$	28.2	10	M (sh)	28.1	a = 32.4_5 Å
	16.2	11	W (sh)	16.2	S = 912 Å^2
	14.0	20	M (sh)	14.0_5	V_{mol} = 3660 Å^3
	10.6	21	M (sh)	10.6	
	7.2	$2h_0$	W (br)	-	
	5.8	h_F+h_H	VS (br)	5.6	
	3.6	h_0	W (br)	4.0	
HBC-$(R_{5,8})_6$	-	10	-	30.8_5	a = 35.6 Å
	17.8_5	11	S (sh)	17.8	S = 1099 Å^2
	15.4	20	VS (sh)	15.4	V_{mol} =3845 Å^3
	11.6	21	S (sh)	11.6_5	
	7.1	$2h_0$	W (br)	-	
	5.6	h_F+h_H	VS (br)	5.5_5	
	3.5	h_0	S (br)	3.5	
HBC-$(R_{6,8})_6$	-	10	-	31.0_5	a = 35.8_5 Å
	17.9_5	11	S (sh)	17.9	S = 1113 Å^2
	15.5	20	VS (sh)	15.5	V_{mol} = 4030 Å^3
	11.6_5	21	S (sh)	11.7_5	
	5.6	h_F+h_H	VS (br)	5.5	
	3.6	h_0	W (br)	3.6	
HBC-$R_{(8,8)_6}$	32.3	10	M (sh)	32.2_5	a = 37.2_5 Å
	18.6	11	S (sh)	18.6	S = 1201 Å^2
	16.1	20	S (sh)	16.1	V_{mol} = 4400 Å^3
	5.5	h_F+h_H	VS (br)	5.4_5	
	3.6	h_0	VW (br)	3.6_5	
HBC-$R_{(4,10)_6}$	13.7	-	S (br)	-	V_{mol} = 4230 Å^3
	5.6	h_F+h_H	S (br)	5.6	
	3.6	h_0	VW (br)	-	
HBC-$R_{(3,1,4)_6}$	27.6_5	10	M (sh)	27.7	T = 140°C
	15.9_5	20	W (sh)	15.9	a = 32.0 Å
	5.5	h_F+h_H	VS (br)	5.4	S = 886 Å^2
	-	-	-	4.5_5	V_{mol} = 4030 Å^3
HBC-$R_{(3,1,6)_6}$	16.2	-	VW (br)	-	T = 100°C
	5.4	h_F+h_H	VS (br)	5.4	
HBC-$R_{(3,2,6)_6}$	14.5	-	VW (br)	-	T = 100°C
	5.3	h_F+h_H	VS (br)	5.3_5	
HBC-$R_{(5,2,6)_6}$	29.4_5	10	M (sh)	29.4_5	T = 60°C
	17.1	11	W (sh)	17.0	a =34.0 Å
	14.6	20	M (sh)	14.7	S = 1001 Å^2
	11.1	21	W (sh)	11.1_5	V_{mol} = 5900 Å^3
	5.2_5	h_F+h_H	VS (br)	5.2	
	-	-	-	5.9	

[a]d_{exp} and d_{theo} are the experimentally measured and calculated diffraction spacings. The distances are given in Å. [b][hk] refer to the indexation of the reflections, and h_0, $2h_0$, h_F , h_H and $h_{F+}h_H$ are the various short range periodicities corresponding to the molecular stacking distance (h_0) and to the average periodicity between liquid-like order of the molten chains ($h_{F+}h_H$), aliphatic chains (h_H) and fluorinated segments (h_F), respectively . [c]Intensity of the reflections: VS: very strong, S: strong, M: medium, W: weak, VW: very weak; br and sh stand for broad and sharp reflections, respectively. [d]d_{theor} and the lattice parameters are deduced from the following mathematical expressions: $a = 2.[\Sigma_{hk}d_{hk}\cdot(h^2+k^2+hk)^{0.5}]/3^{0.5}N_{hk}$ where N_{hk} is the number of hk reflections and the lattice area (i.e.)

columnar cross-section, $S = 3^{0.5}a^2/2$ for Col_h; $<d_{hk}> = 1/[(h^2/a^2+k^2/b^2)^{0.5}]$, and the lattice area S = ½. a×b for Col_{hr}. $^eV_{mol}$ is the molecular volume: $V_{mol} = V_{HBC} + 6(nV_{CH2} + mV_{CF2})$, where V_{HBC} = 650 Å^3, $V_{CH2} = 26.5616 + 0.02023T$ (30.6076 Å^3 at 200 °C), and $V_{CF2} = 40.815 + 0.03318T$ (47.451 Å^3 at 200 °C); $h = h_0$(theor) is the theoretical intracolumnar repeating distance, deduced directly from the measured molecular volume and the columnar cross-section according to $h = V_{mol}/S$; h_F+h_H(theor) = $[(n.h_H.\sigma_H)+(m.h_F.\sigma_F)]/[n.\sigma_H+m.\sigma_F]$, where $h_H = 0.9763.\sigma_H^{½}$ = 4.8 Å (at T = 200°C), $h_F = 0.9763.\sigma_F^{½}$ = 5.85 Å (at T = 200°C), and $\sigma_{H/F}$ are the chain-cross section (hydrogenated and fluorinated segments, respectively), defined as $\sigma_H = V_{CH2}/1.27$ and $\sigma_F = V_{CF2}/1.32$. For the branhced derivatives: h_H = 4.7, 4.63 and 4.56 Å (at T = 140, 100 and 60°C), h_F = 5.72, 5.64, 5.56 Å (at T = 140, 100 and 60°C)[1].

[1] Marcos, J.; Giménez, R.; Serrano, J.-L.; Donnio, B.; Heinrich, B.; Guillon, D. Chem. Eur. J., 7 (2001), 1006-1013.

Table S2. Parameters used for the density reconstruction charts[a]

T = 200	$(CH_2)n$	a	h	V_{HBC}	V_{ch}	D_c	D_{c+ch}	D_c/a%	D_{c+ch}/a%	D1	D2
HBC-$(R_{4,4})_6$	4	26.6	4.1	650	734.58	14.208	20.736	53.412	77.954	274	400
HBC-$(R_{2,6})_6$	2	28.7_5	3.8	650	367.29	14.758	18.462	51.331	64.217	262	328
HBC-$(R_{3,6})_6$	3	31.0	3.5	650	550.94	15.377	20.902	49.604	67.425	254	346
HBC-$(R_{4,6})_6$	4	31.4	3.6	650	734.58	15.162	22.129	48.287	70.475	248	360
HBC-$(R_{5,6})_6$	5	33.6	3.3_5	650	918.23	15.718	24.414	46.779	72.660	240	372
HBC-$(R_{6,6})_6$	6	33.5	3.5_5	650	1101.87	15.247	25.031	45.514	74.720	234	382
HBC-$(R_{3,8})_6$	3	33.7	3.5	650	550.94	15.421	20.962	45.761	62.201	234	318
HBC-$(R_{4,8})_6$	4	32.4_5	4.0	650	734.58	14.384	20.993	44.327	64.695	226	332
HBC-$(R_{5,8})_6$	5	35.6	3.5	650	918.23	15.377	23.885	43.194	67.093	222	344
HBC-$(R_{6,8})_6$	6	35.8_5	3.6	650	1101.87	15.162	24.892	42.293	69.433	216	356
HBC-$R(_{8,8})_6$	8	37.2_5	3.6_5	650	1469.16	15.037	27.152	40.369	72.890	206	374

[a]Volume of the aliphatic chain- segments: $V_{ch} = 30.6076 \times n \times 6$; Diameter of the hard columnar core: $D_c = \sqrt{(4 \times V_{HBC}/\pi \times h)}$ (D_{in}); Diameter of the aliphatic enveloppe: $D_{c+ch} = \sqrt{(4 \times (v_{HBC}+v_{ch})/ \pi \times h)}$ (D_{out}); Proportion relative to a, the intercolumnar distance: $D_c/a\% = 100 \times D_c/a$, and $(D_{c+ch})/a\% = 100 \times (D_{c+ch})/a$; Normalisation to pixel definition: D_1 ring $= 512 \times D_c/100$, D_2 ring $= 512 \times (D_{c+ch})/100$, D_1, intern cylinder diameter, and D_2, outer cylinder diameter.

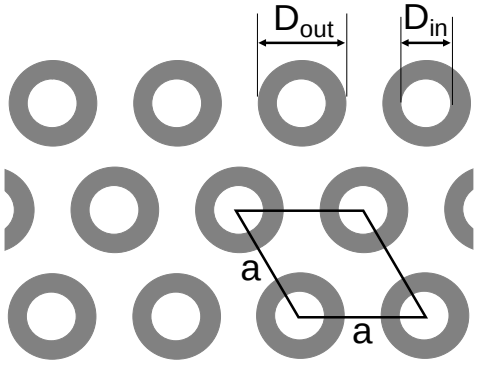

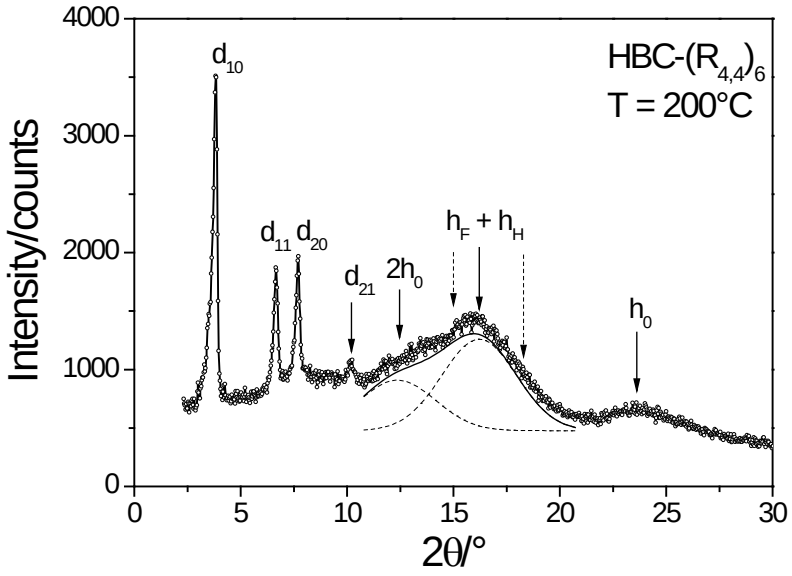
HBC-(R4,4)6
T = 200°C
d10
d11 d20
d21
2h0
hF + hH
h0
Intensity/counts
2θ/°
0
1000
2000
3000
4000
0
5
10
15
20
25
30

A

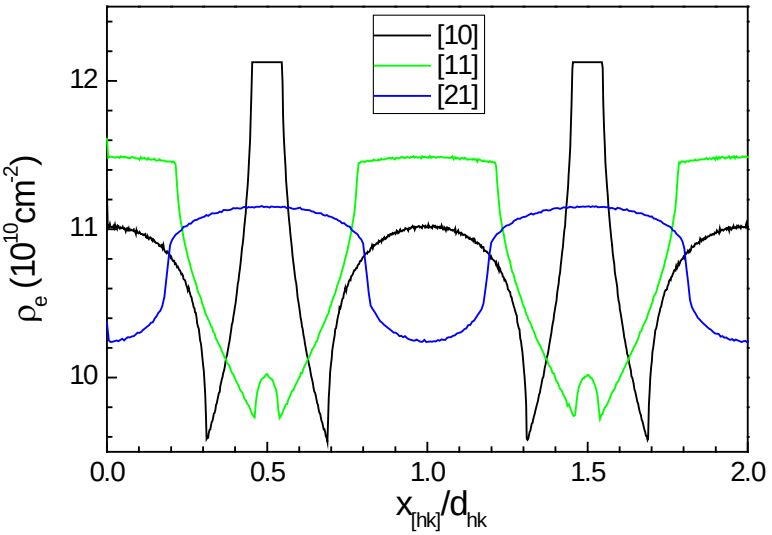
[10]
[11]
[21]
ρe (10^10 cm^-2)
x[hk]/dhk
10
11
12
0.0
0.5
1.0
1.5
2.0

B

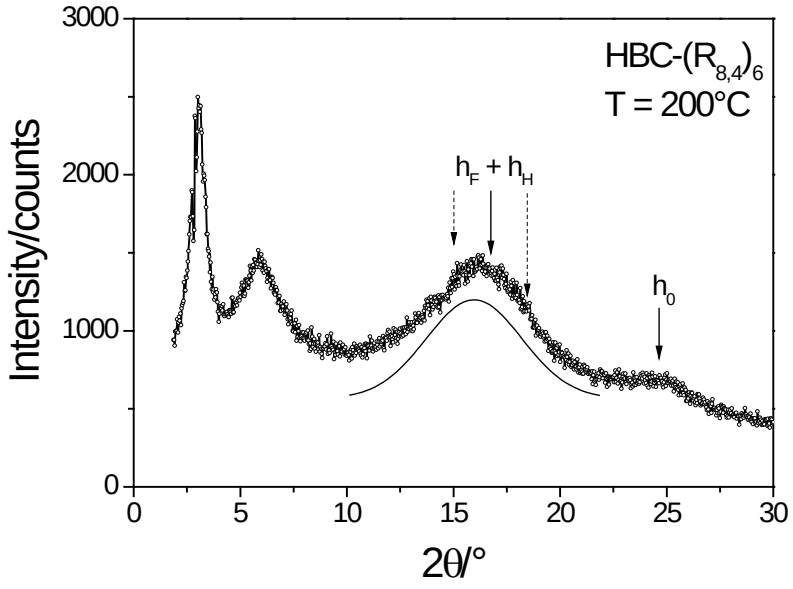
HBC-(R8,4)6
T = 200°C
hF + hH
h0
Intensity/counts
2θ/°
0
1000
2000
3000
0
5
10
15
20
25
30

A

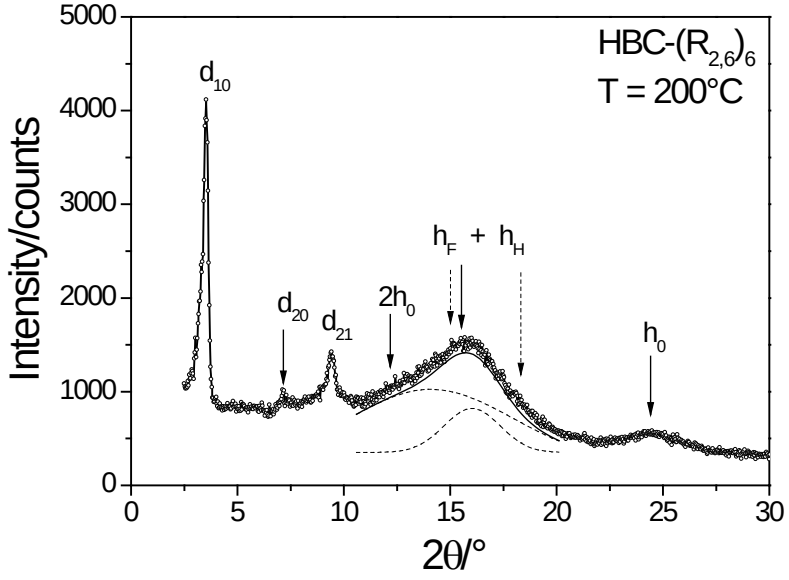
HBC-(R2,6)6
T = 200°C
d10
d20
d21
2h0
hF + hH
h0
Intensity/counts
2θ/°
0
1000
2000
3000
4000
5000
0
5
10
15
20
25
30

A

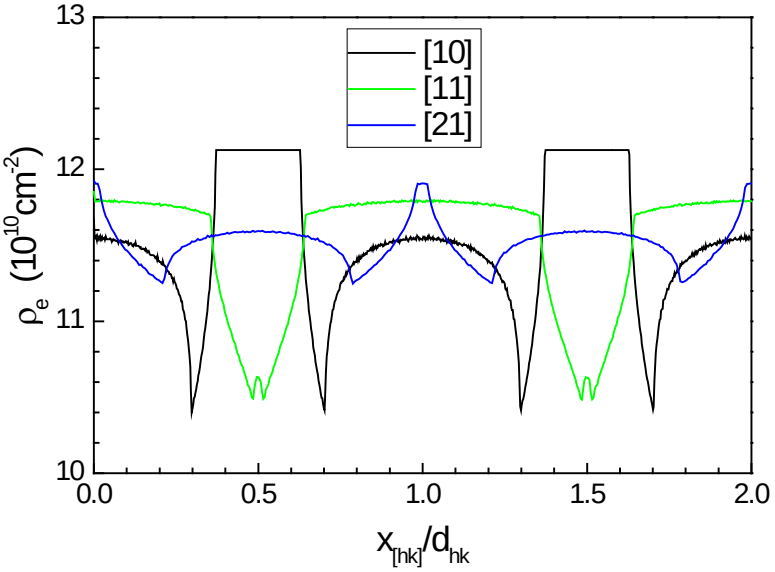
[10]
[11]
[21]
ρe (10^10 cm^-2)
x[hk]/dhk
10
11
12
13
0.0
0.5
1.0
1.5
2.0

B

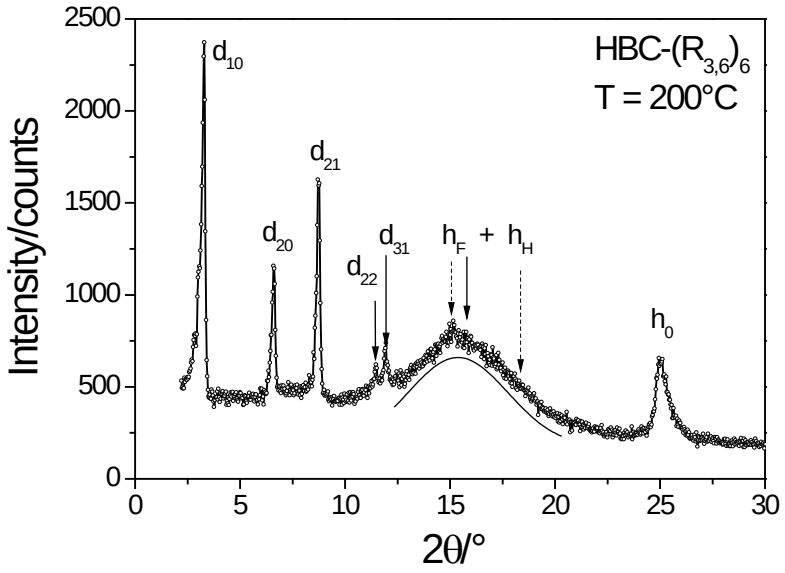
HBC-(R3,6)6
T = 200°C
d10
d20
d21
d22
d31
hF + hH
h0
Intensity/counts
2θ/°
0
500
1000
1500
2000
2500
0
5
10
15
20
25
30

A

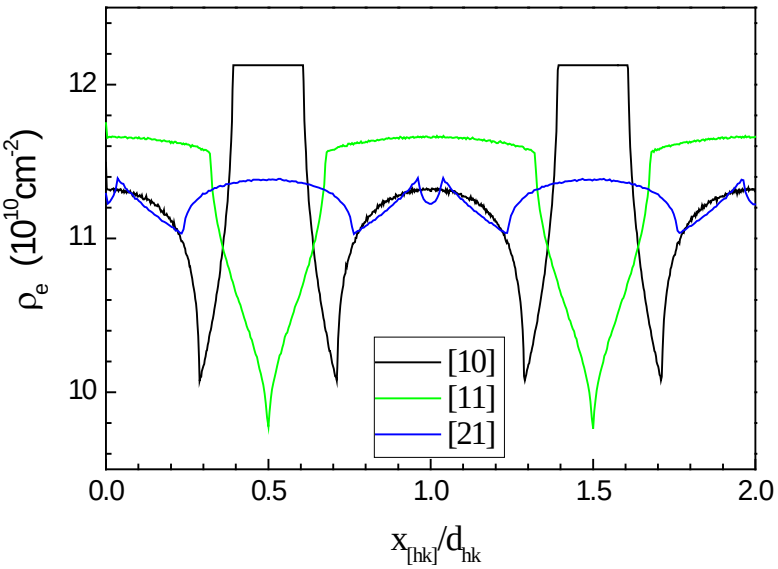
[10]
[11]
[21]
ρe (10^10 cm^-2)
x[hk]/dhk
10
11
12
0.0
0.5
1.0
1.5
2.0

B

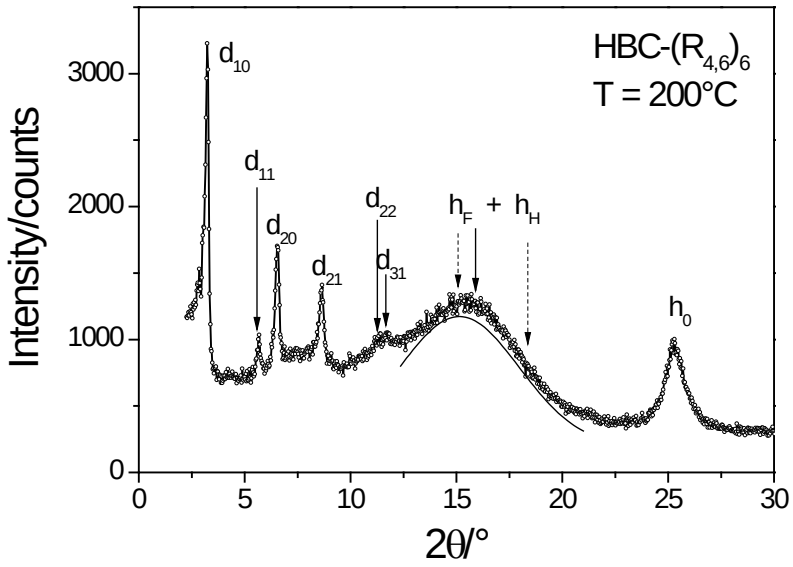

A[2]

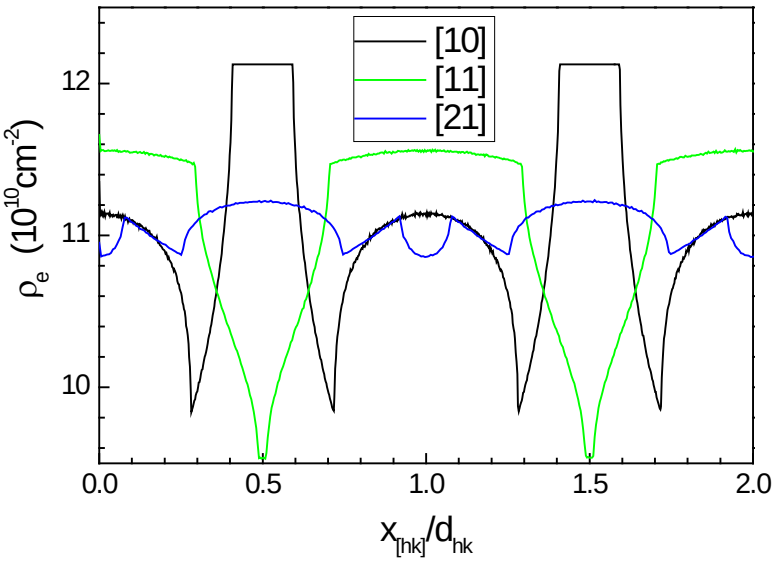

B

[2] Aebischer, O. F.; Aebischer, A.; Donnio, B.; Alameddine, B.; Dadras, M.; Güdel, H.-U.; Guillon, D.; Jenny, T. A. *J. Mat. Chem.* **2007**, *17*, 1262-1267.

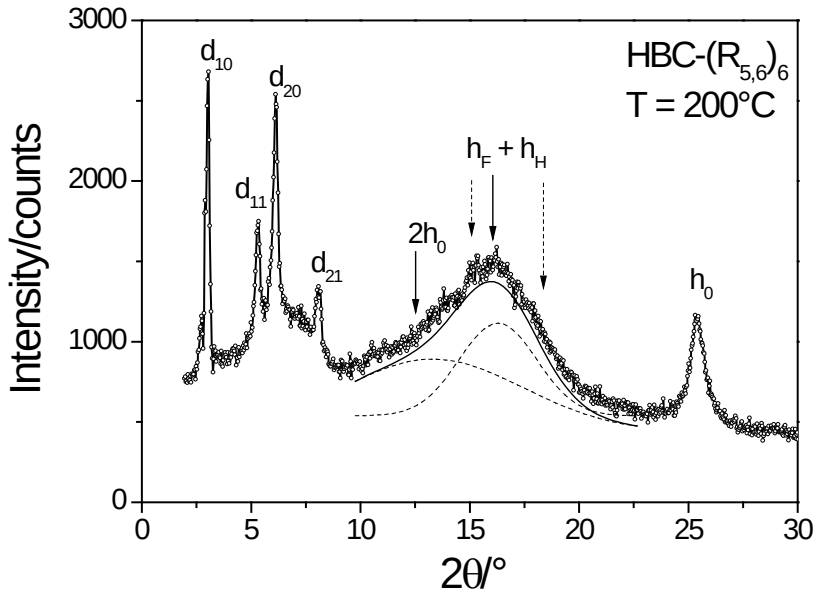
HBC-(R5,6)6
T = 200°C
d10
d20
d11
d21
2h0
hF + hH
h0
Intensity/counts
2θ/°
0
1000
2000
3000
0
5
10
15
20
25
30

A

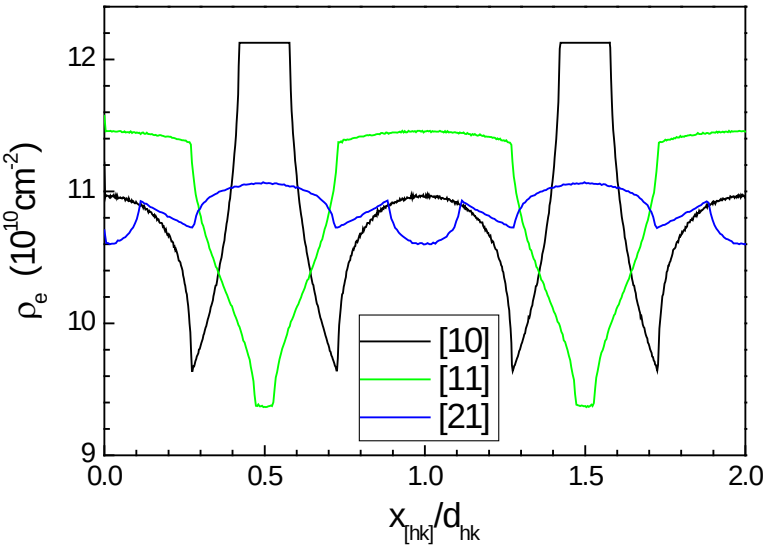
[10]
[11]
[21]
ρe (10^10 cm^-2)
x[hk]/dhk
9
10
11
12
0.0
0.5
1.0
1.5
2.0

B

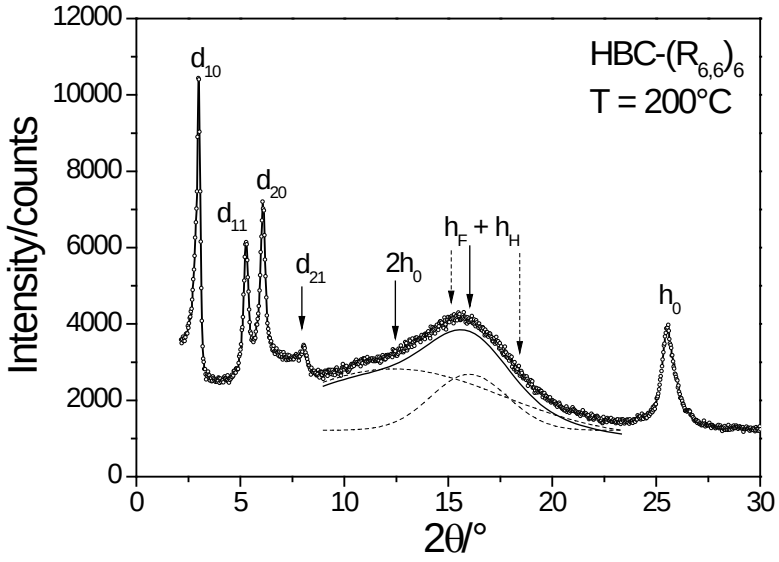

A[3]

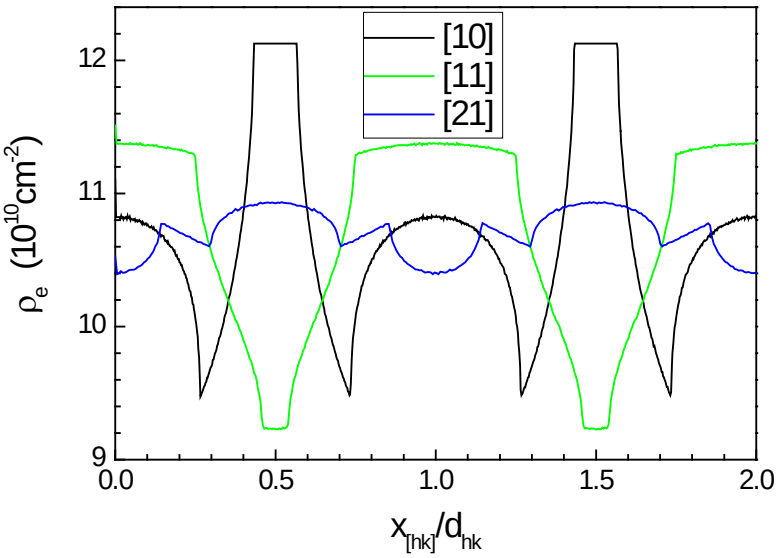

B

[3] Alameddine, B.; Aebischer, O. F.; Amrein, W.; Donnio, B.; Deschenaux, R.; Guillon, D.; Savary, C.; Scanu, D.; Scheidegger, O.; Jenny, T. A. *Chem. Mater.* **2005**, *17*, 4798-4807.

HBC-$(R_{8,6})_6$

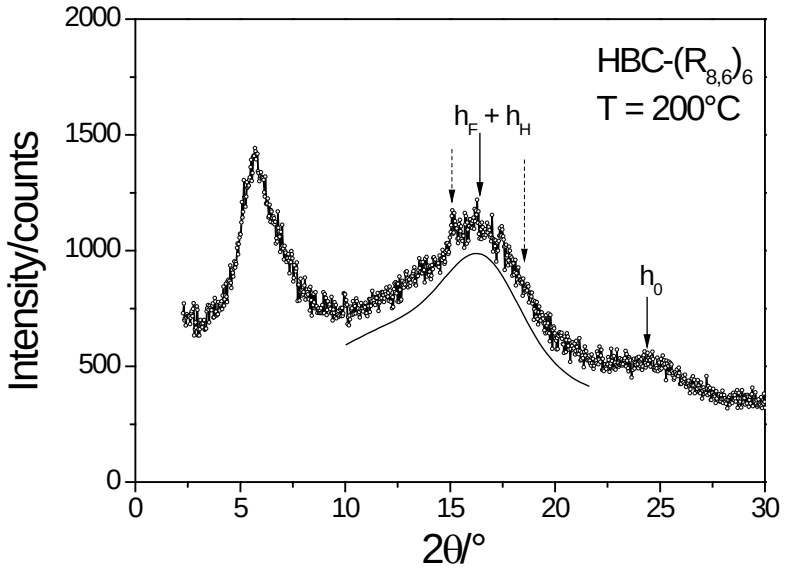
HBC-(R8,6)6
T = 200°C
hF + hH
h0
Intensity/counts
2θ/°
0
500
1000
1500
2000
0
5
10
15
20
25
30

A

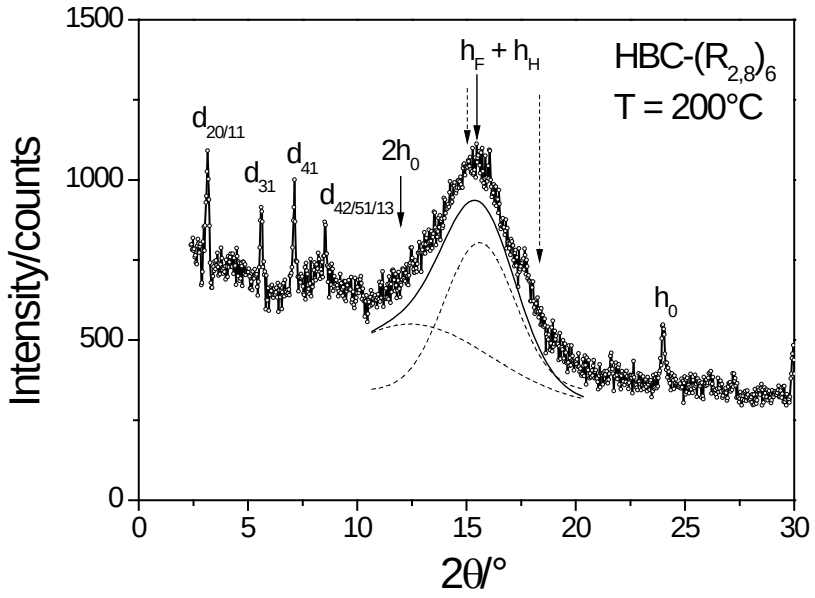
1500
1000
500
0
Intensity/counts
0
5
10
15
20
25
30
2θ/°
$h_F + h_H$
HBC-$(R_{2,8})_6$
T = 200°C
$d_{20/11}$
d_{31}
d_{41}
$d_{42/51/13}$
$2h_0$
h_0

A

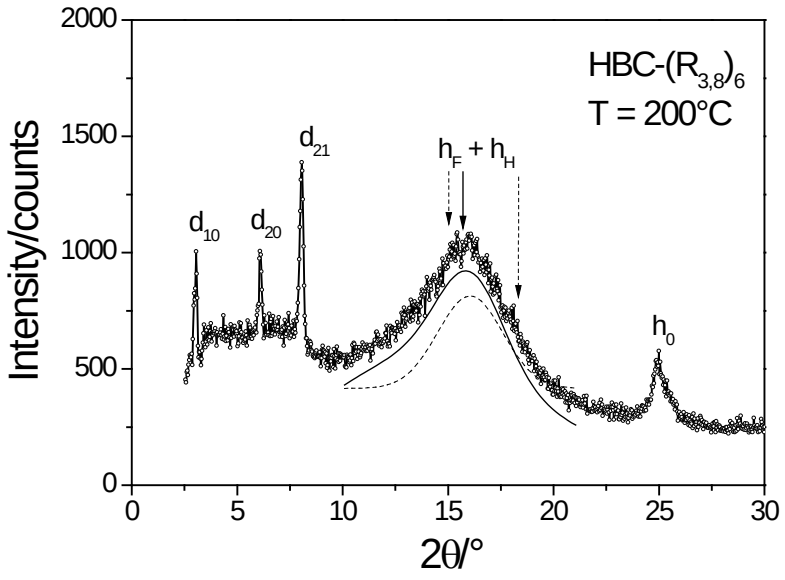
HBC-(R3,8)6
T = 200°C
Intensity/counts
2θ/°
d10
d20
d21
hF + hH
h0
0
500
1000
1500
2000
0
5
10
15
20
25
30

A

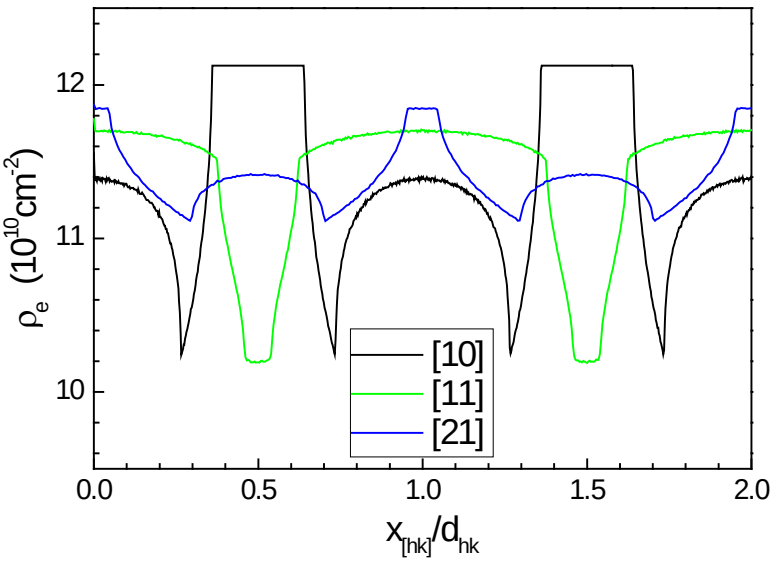
ρe (10^10 cm^-2)
x[hk]/dhk
[10]
[11]
[21]
10
11
12
0.0
0.5
1.0
1.5
2.0

B

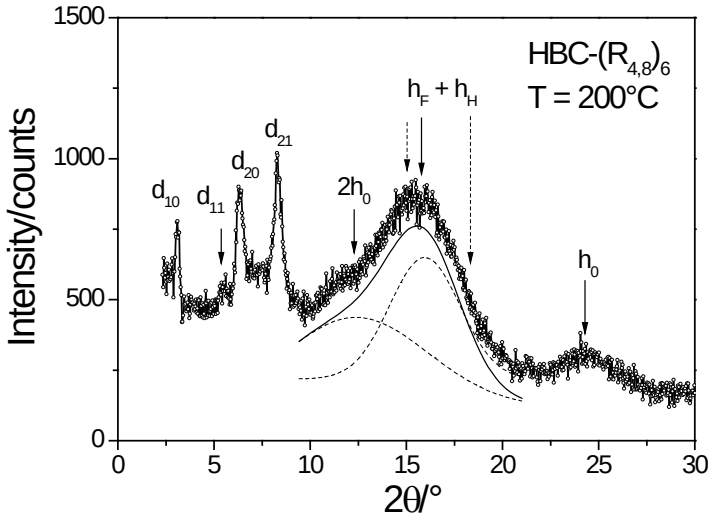

A[4]

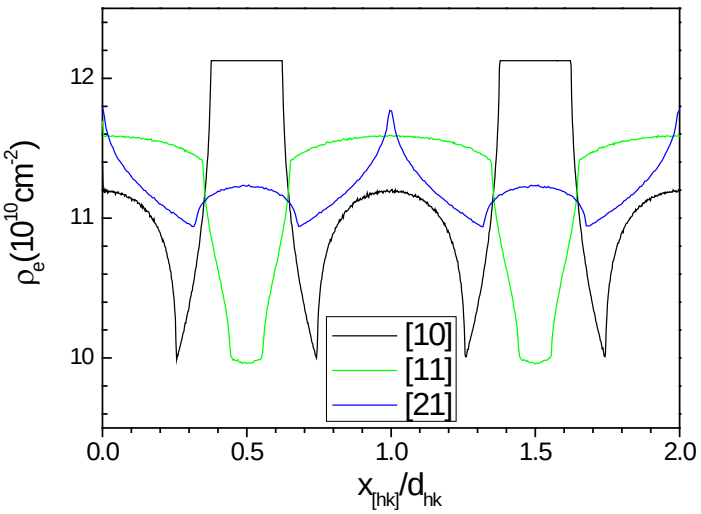

B

[4] Alameddine, B.; Aebischer, O. F.; Amrein, W.; Donnio, B.; Deschenaux, R.; Guillon, D.; Savary, C.; Scanu, D.; Scheidegger, O.; Jenny, T. A. *Chem. Mater.* **2005**, *17*, 4798-4807.

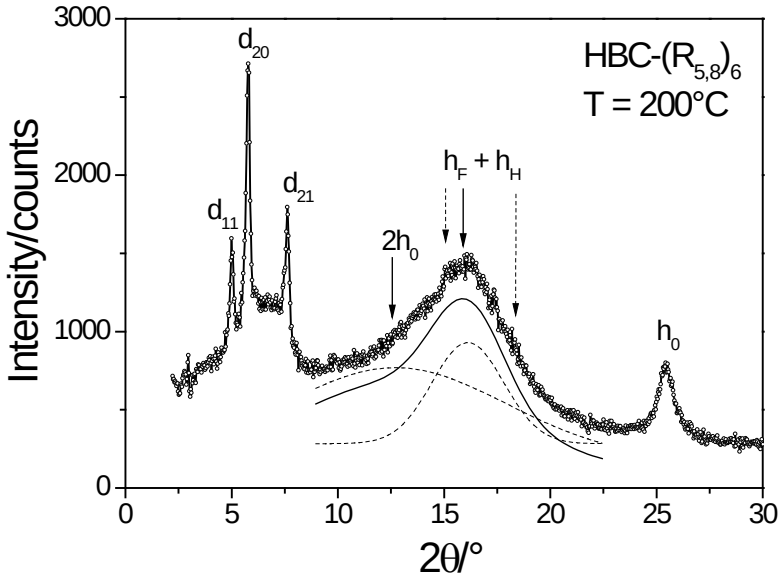
HBC-(R5,8)6
T = 200°C
d20
d11
d21
2h0
hF + hH
h0
Intensity/counts
2θ/°
0
1000
2000
3000
0
5
10
15
20
25
30

A

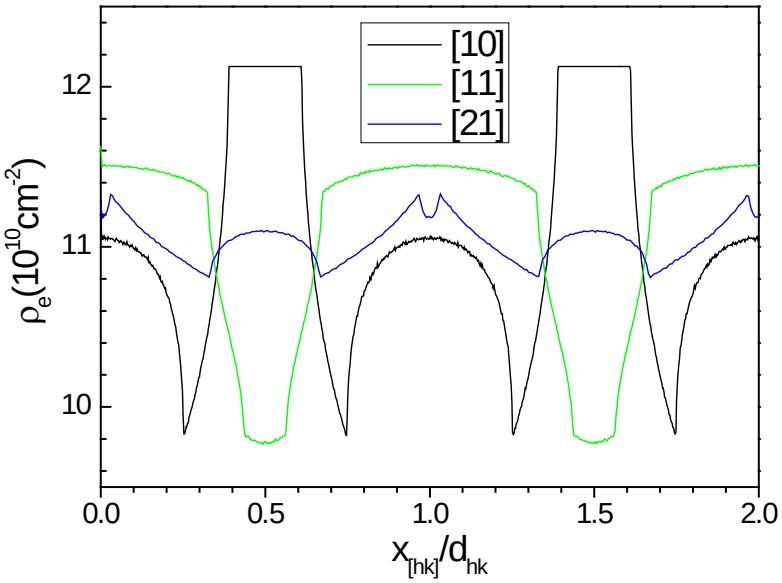
[10]
[11]
[21]
ρe(10^10cm^-2)
x[hk]/dhk
10
11
12
0.0
0.5
1.0
1.5
2.0

B

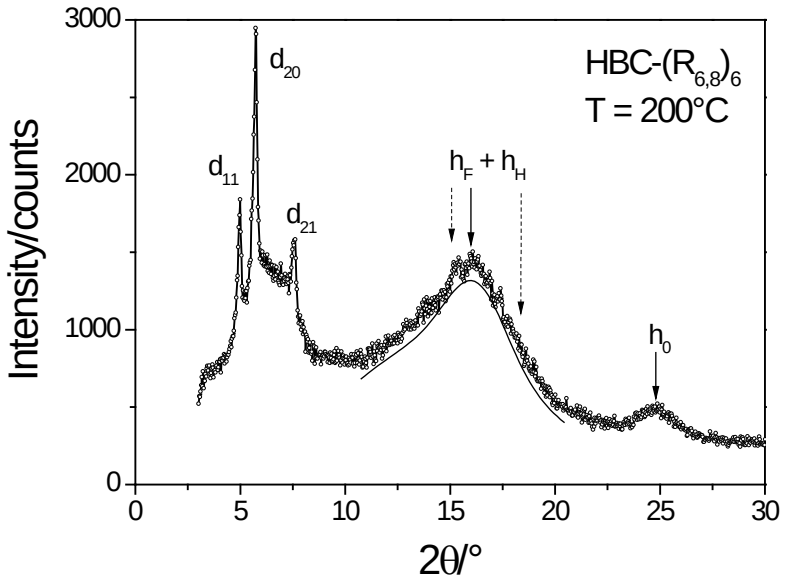
HBC-(R6,8)6
T = 200°C
d20
d11
d21
hF + hH
h0
Intensity/counts
2θ/°
0
1000
2000
3000
0
5
10
15
20
25
30

A

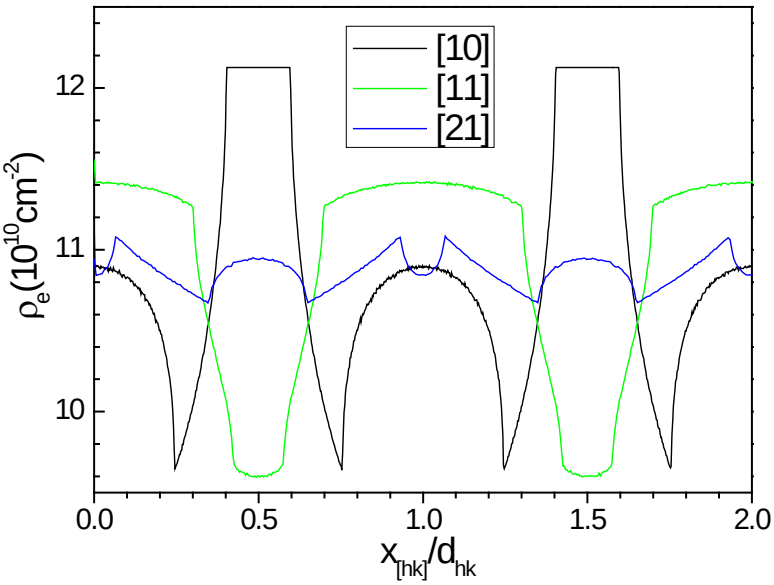
[10]
[11]
[21]
ρe(10^10cm^-2)
x[hk]/dhk
10
11
12
0.0
0.5
1.0
1.5
2.0

B

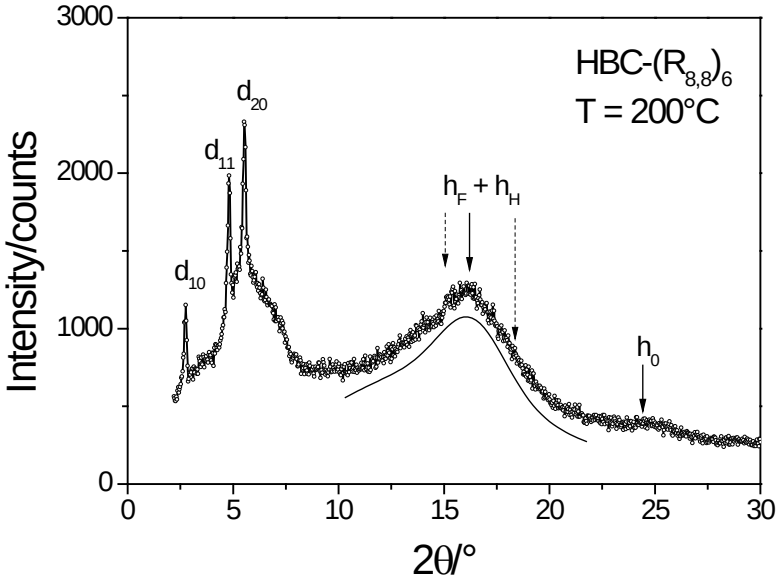
HBC-(R8,8)6
T = 200°C
d10
d11
d20
hF + hH
h0
Intensity/counts
2θ/°
0
1000
2000
3000
0
5
10
15
20
25
30

A

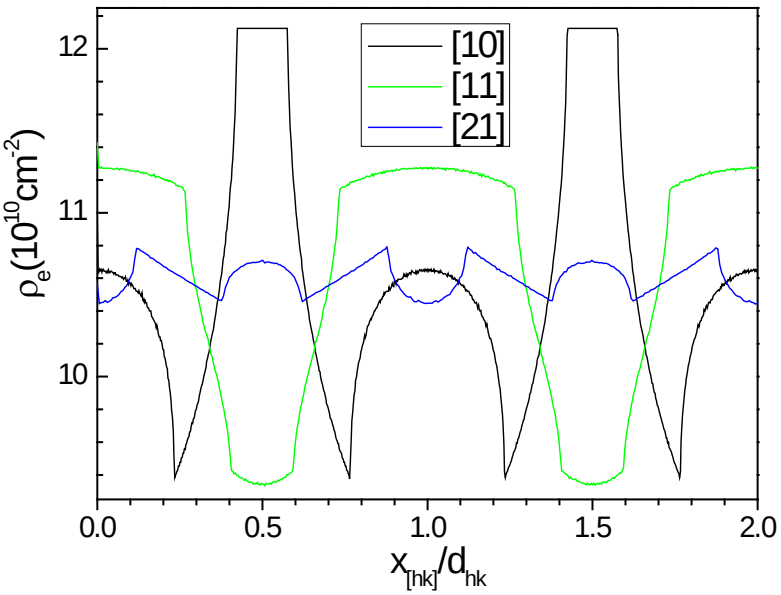
[10]
[11]
[21]
ρe(10^10cm^-2)
x[hk]/dhk
10
11
12
0.0
0.5
1.0
1.5
2.0

B

HBC-R$(_{4,10})_6$

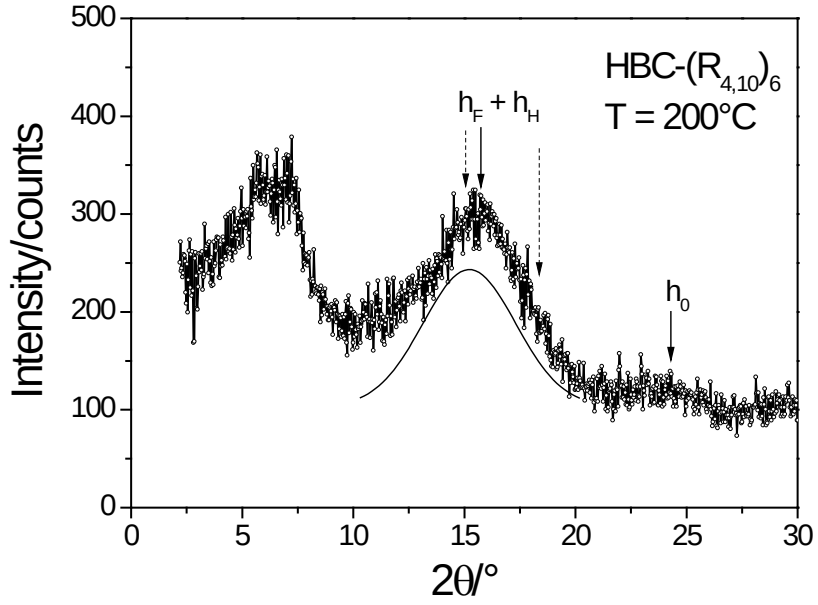
HBC-(R4,10)6
T = 200°C
hF + hH
h0
Intensity/counts
2θ/°
0
100
200
300
400
500
0
5
10
15
20
25
30

A

Simulation of the electronic density in the classical case of disc with alkylated chains

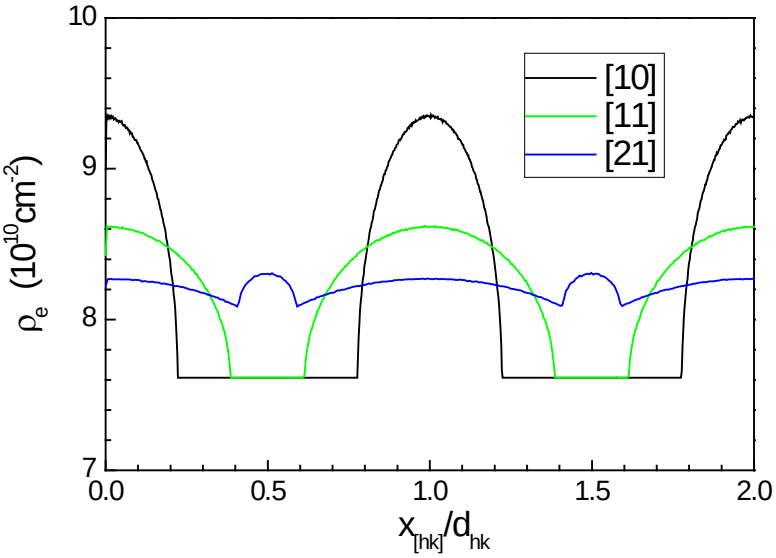

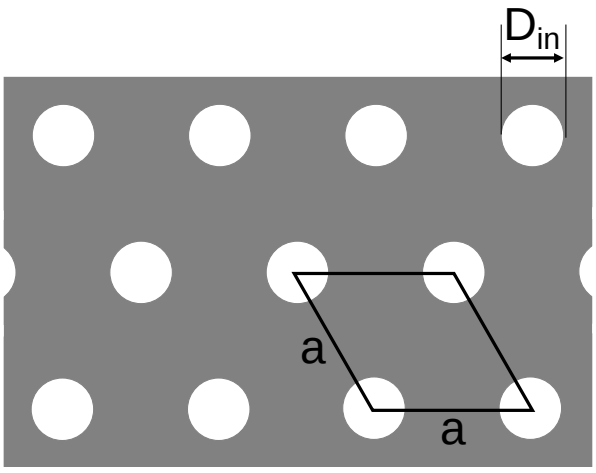

HBC derivatives with branched semi-perfluorinated chains

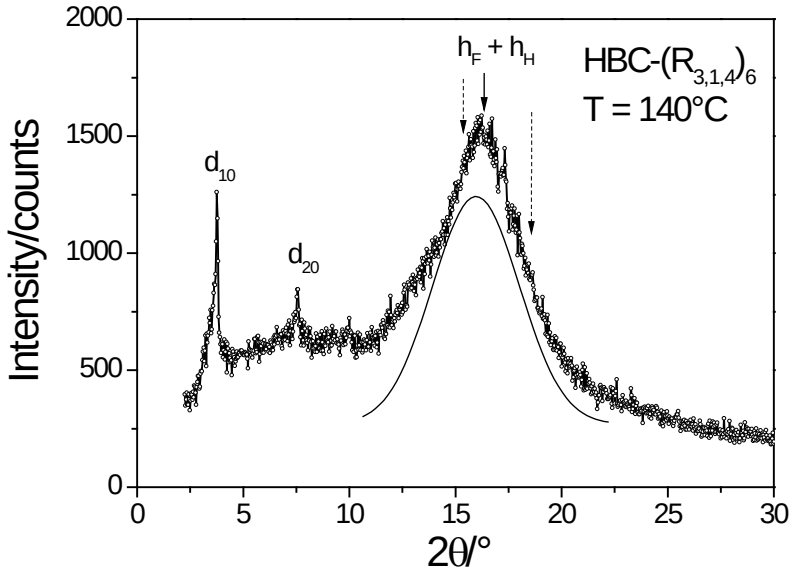

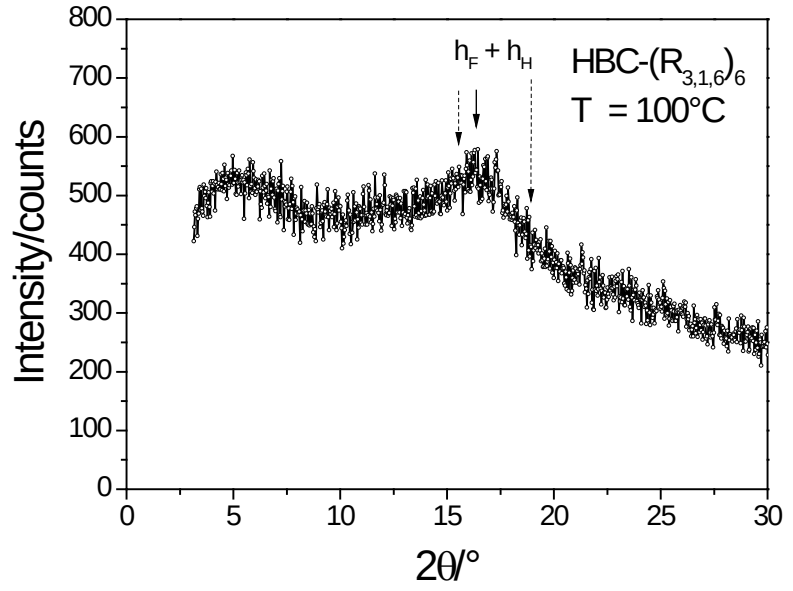

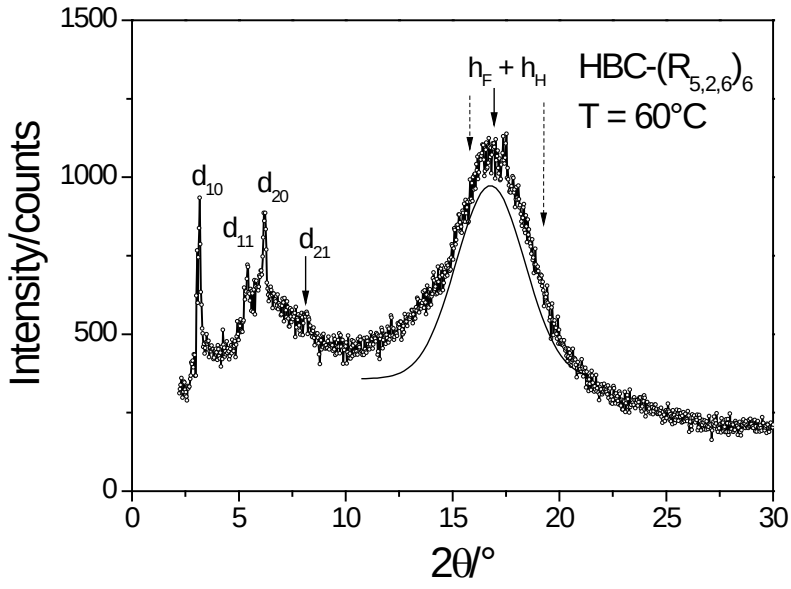
1500
1000
500
0
Intensity/counts
0
5
10
15
20
25
30
2θ/°
h_F + h_H
HBC-(R_5,2,6)_6
T = 60°C
d_10
d_20
d_11
d_21

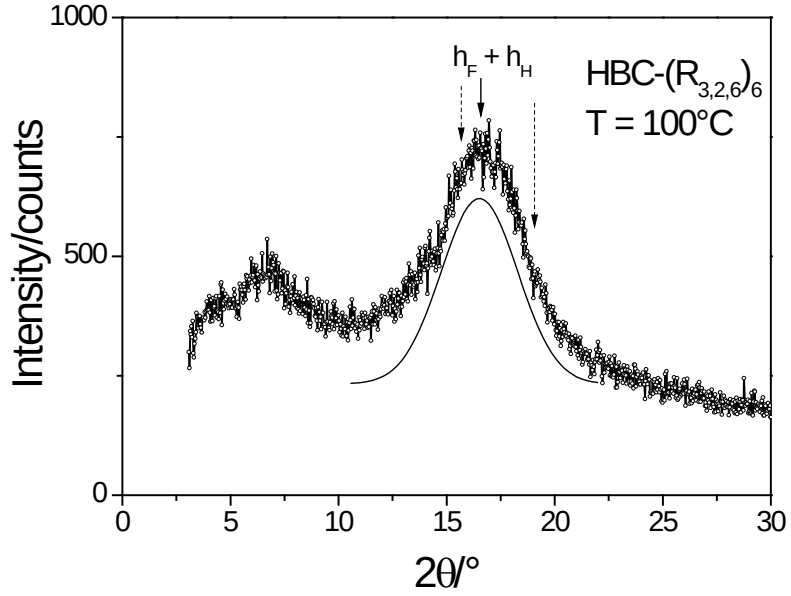
1000
500
0
Intensity/counts
0
5
10
15
20
25
30
2θ/°
h_F + h_H
HBC-(R_3,2,6)_6
T = 100°C

Thermogravimetry (TGA)

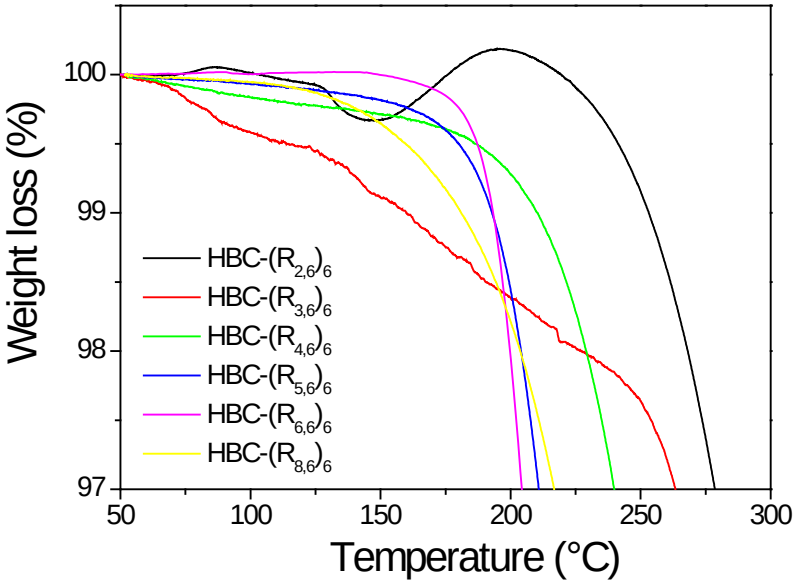

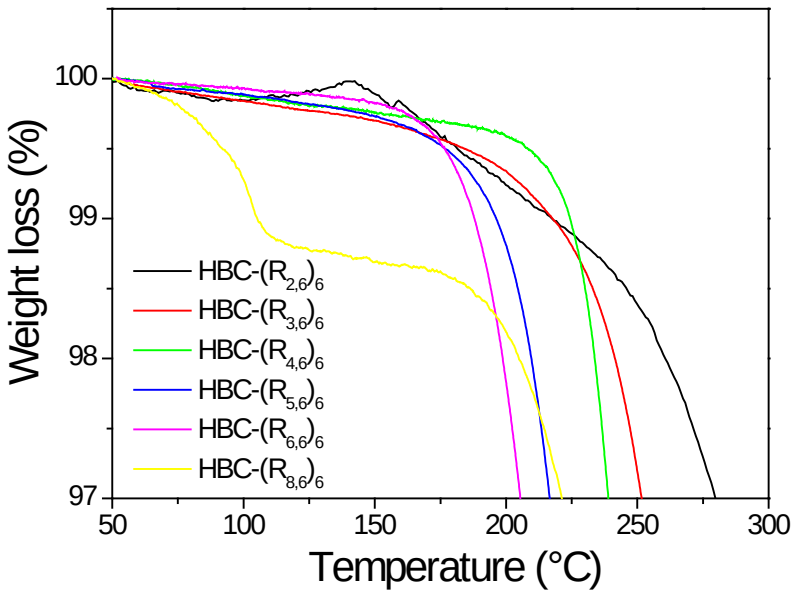

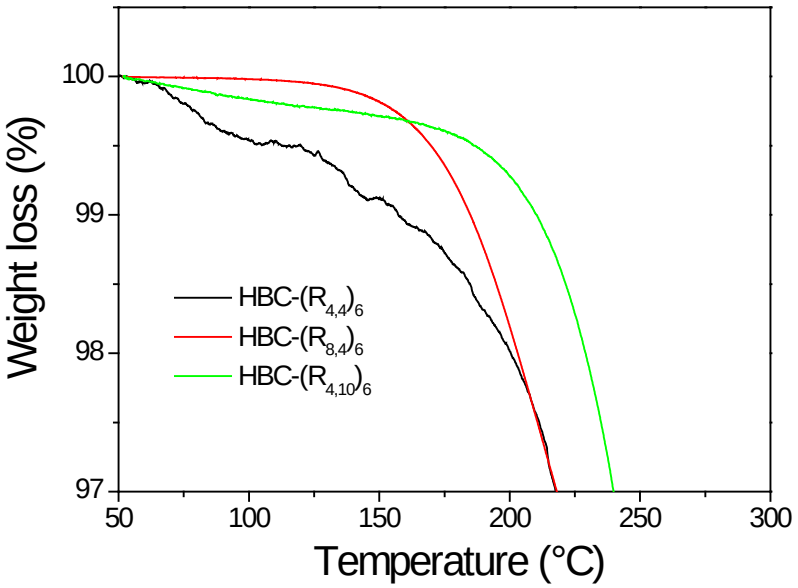
Weight loss (%)
100
99
98
97
50
100
150
200
250
300
Temperature (°C)
HBC-(R4,4)6
HBC-(R8,4)6
HBC-(R4,10)6

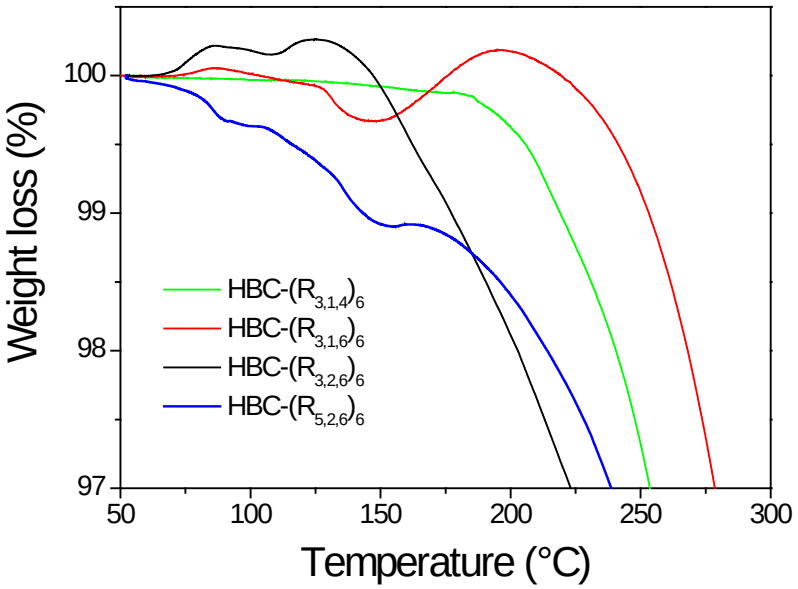
Weight loss (%)
100
99
98
97
50
100
150
200
250
300
Temperature (°C)
HBC-(R3,1,4)6
HBC-(R3,1,6)6
HBC-(R3,2,6)6
HBC-(R5,2,6)6

Molecular dynamic simulation for HBC-$(R_{4,6})_6$, showing the alternated stacking of the HBC derivative to fill the entire accessible volume between discs and columns[5].

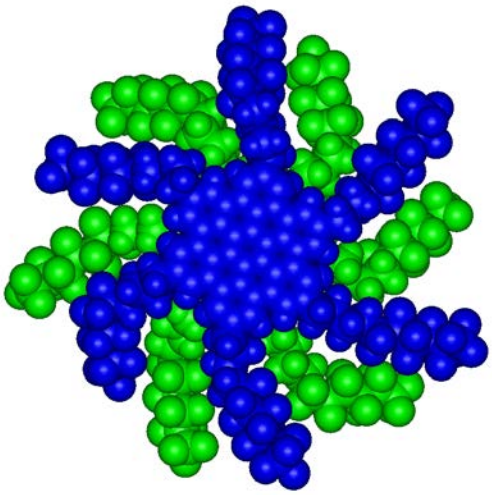

Top view

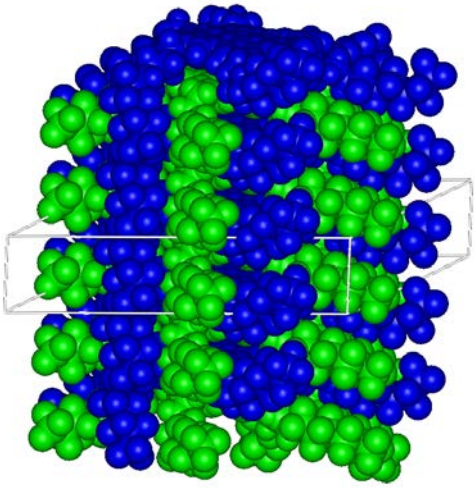

Side view

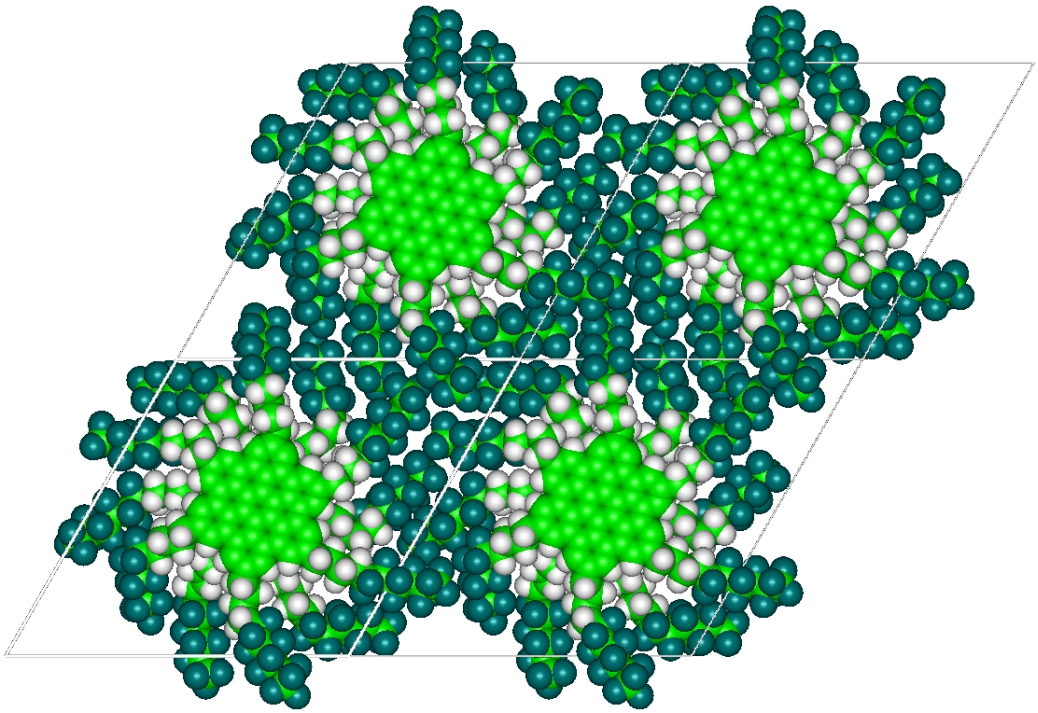

Hexagonal lattice

[5] Aebischer, O. F.; Aebischer, A.; Donnio, B.; Alameddine, B.; Dadras, M.; Güdel, H.-U.; Guillon, D.; Jenny, T. A. *J. Mat. Chem.* **2007**, *17*, 1262-1267.

Cryo-SEM

The described derivatives exhibit upon heating a mesophase preceded by a crystalline phase or are amorphous at all temperatures. The organization in the mesophase was highlighted by powder XRD, but the crystalline structures were not resolved, although both types of organizations should be closely connected. The search of complementary information motivated us to resort to Cryo-SEM, as reported previously to illustrate the self-assembly of disc-shaped perfluorinated HBCs.

In order to obtain a consistent picture, these experiments were performed with the same solvent as the one used to precipitate the samples for XRD measurements, i.e.-trifluoromethyl benzene (BTF). As a matter of fact, the self-aggregation of these structures was shown to be highly dependent on the nature of the solvent and the concentration of the medium. Therefore the concentration of the solutions in BTF (a solvent of intermediate solubilizing capacity for these compounds) was fixed to 10^{-4} M. The cryo-SEM investigation was carried out using the HBC derivatives bearing linear chains with four methylene spacers (HBC-$(R_{4,4})_6$, **1a**, HBC-$(R_{4,6})_6$, **2c**, HBC-$(R_{4,8})_6$, **3c**, and HBC-$(R_{4,10})_6$, **4a**) and four HBC derivatives with branched chains (HBC-$(R_{3,1,4})_6$, **5a**, HBC-$(R_{3,1,6})_6$, **5b**, HBC-$(R_{3,2,6})_6$, **5c**, and HBC-$(R_{5,2,6})_6$, **5d**). Characteristic pictures are shown in Figure S8.

Under cryo-SEM conditions HBC-$(R_{4,4})_6$, **1a**, produces large, nearly cylindrical assemblies with a typical length of 20 μm and a diameter of ~1 μm. However, these structures taper off at their ends fraying into smaller thin sheets, typically 200 nm wide. These thin sheets are most probably the basic architectures from which the large cylindrical structures form by aggregation.

Similarly, HBC-$(R_{4,6})_6$, **2c**, produces large aggregated sheets and bundles with similar dimensions as compared to those observed for HBC-$(R_{4,4})_6$, **1a**. Surprisingly, HBC-$(R_{4,8})_6$, **3c**, forms much finer structures than the other derivatives under these conditions. These fibers were

found to have variable lengths ranging from 1 to 30 μm at a uniform cross-section of roughly 200 nm. The filamentous linear structures were found to completely cover the surface of the frozen solvent indicating that the equilibrium among the various forms of aggregation (monomer, oligomer, single stranded stacks, laterally aggregated single strands etc.) was highly shifted favoring the formation of these structures. HBC-$(R_{4,10})_6$, **4a**, was the only derivative within this series that did not show linear structures. Instead, a number of droplet-like aggregates with diameters ranging between 200 and 800 nm were observed.

Cryo-SEM investigation revealed a rather similar behaviour among all four branched HBC derivatives. Thread-like linear structures were found combined with round or oval shaped structures. This feature is most pronounced in the case of HBC-$(R_{5,2,6})_6$, **5d**, where cocoon-like structures (~250 nm long, ~170 nm wide) seem suspended within entangled filaments (diameter ~60 nm) bestowing the material with a cobweb-like appearance. As the aliphatic spacer shortens in HBC-$(R_{3,2,6})_6$, **5c**, the filamentous sections become less frequent while increasing their thickness before disappearing nearly totally in HBC-$(R_{3,1,6})_6$, **5b**. Finally the compound with the shortest branched side chains and a reduced fluorine content, HBC-$(R_{3,1,4})_6$, **5a**, exhibits an amorphous shape much more reminiscent on oily droplets than an ordered structure. In this regard this compound somehow compares to the linear side chain compound with the highest fluorine content, HBC-$(R_{4,10})_6$, **4a**, which shows unlike the other compounds with linear side chains no filamentous structure at all.

The cryo-SEM results for these HBC derivatives bearing linear perfluoroalkylated chains evidently corroborate with the powder XRD data. The mesomorphic columnar hexagonal packing detected by XRD is revealed in the Cryo-SEM sample by an ordered pattern, which could be interpreted as columnar structures of self-assembled HBC molecules closely packed into thin sheets and these sheets piled up like in stack of paper. The powder XRD of HBC-$(R_{4,10})_6$, **4a**, however shows only diffuse reflexes for the core structures, very much in line with the cryo-SEM picture of this compound.

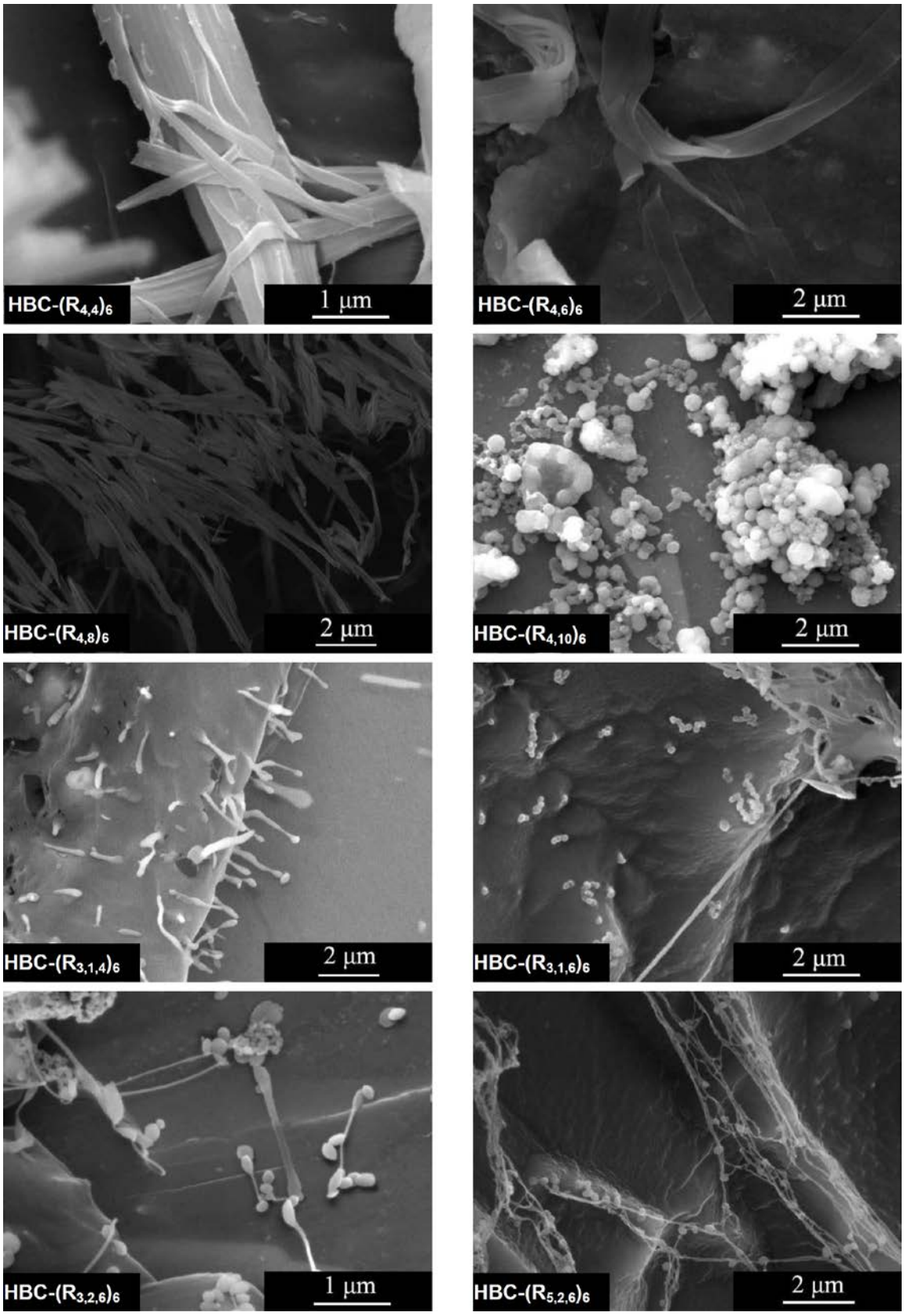

Figure S8. cryo-SEM images from representative HBC derivatives in 10^{-4}M BTF solutions.